

Vikram K. Daga
Norman J. Wagner

Linear viscoelastic master curves of neat and laponite-filled poly(ethylene oxide)–water solutions

Received: 11 February 2005
Accepted: 25 October 2005
Published online: 11 January 2006
© Springer-Verlag 2006

Abstract Aqueous solutions composed of dispersed nanoparticles and entangled polymers are shown to exhibit common viscoelasticity over a range of particle and polymer concentrations. Time–temperature superposition and time–concentration superposition are applied to generate rheological master curves for neat and laponite-filled aqueous solutions of poly(ethylene oxide). The shift factors were correlated in terms of temperature and concentration and are found to differ from previous reports for ideal polymer solutions, which can be rationalized with a molecular interpretation of the structure of the laponite–polymer solutions. Laponite addition to the concentrated polymer solution is observed to increase the relaxation time but decrease the elastic modulus, which is a consequence of polymer adsorption and bridging. The addition of small amounts of laponite to stable PEO–water solutions also leads to ageing on the time scale of days.

Keywords Nanocomposite · Polymer solution · Laponite · Nanoparticle · Time–temperature superposition · Time–concentration superposition · Master curve · Ageing · Viscoelasticity · Adsorption · Entanglement density

Abbreviations PEO: Poly(ethylene oxide) · PW: PEO–water solution · PWL: PEO–water–laponite mixture · TTSP: Time–temperature superposition · TCSP: Time–concentration superposition · P : Weight percent of PEO in PWL mixture · W : Weight percent of water in PWL mixture · L : Weight percent of laponite in PWL mixture · c : Weight percent of PEO in aqueous solution · η : Viscosity (Pa s) · $\dot{\lambda}$: Shear rate (s^{-1}) · ρ : Density (g/cm^3) · ω : Angular frequency (rad/s) · G' : Storage modulus (Pa) · G'' : Loss modulus (Pa) · a_T : Horizontal time–temperature shift factor · b_T : Vertical time–temperature shift factor · a_c : Horizontal time–concentration shift factor · b_c : Vertical time–concentration shift factor · T : Temperature · g_i : Relaxation strength (Pa) · λ_i : Relaxation time (s) · s : Specific surface area of laponite provided for PEO adsorption (m^2/mg PEO) · Subscripts— g : Glass transition · ref : Reference · θ : Zero–shear · 1 and 2: Level of TCSP in case of PWL mixtures

V. K. Daga · N. J. Wagner (✉)
Center for Molecular
and Engineering Thermodynamics,
Department of Chemical Engineering,
University of Delaware,
Newark, DE 19716, USA
e-mail: wagner@che.udel.edu
Tel.: +302-8318079
Fax: +302-8311048

Present address:
V. K. Daga
Hindustan Lever Limited,
165/166 Backbay Reclamation,
Mumbai 400020, India

Introduction

Polymer–clay nanocomposites exhibiting superior properties find applications in various commercial products in the agricultural (Greenblatt et al. 2004; Theng 1970), pharmaceutical (Greenblatt et al. 2004; Wong 2004), electrochemical (Aranda et al. 2003; Doeff and Reed 1998; Feller et al. 2004), photochemical (Majumdar et al. 2003) and personal care (Sengupta et al. 2002; Smith et al. 1989) industries. The final material properties of such composites are often highly

dependent on their processing history due to the strong coupling between the nanocomposite's microstructure and rheology. Hence, it is of importance to establish the rheological effects associated with the addition of nanoparticles to polymers and polymer solutions.

For example, one application attracting recent research interest is the electrospinning of polymeric materials to produce nanoscale fibers (Casper et al. 2004; Huang et al. 2003; Jayaraman et al. 2004; Megelski et al. 2002). Colloidal particles have been incorporated within the electro-

spun fibers for such purposes as to enhance the mechanical properties of the electrospun fibers (Krikorian et al. 2004) and to generate high specific surface area catalytic particles (Drew et al. 2003). The rheology of the spinning solution is known to affect the fiber diameter (McKee et al. 2004). Consequently, the rational design and control of the electrospinning process requires knowledge of the rheological properties of the spinning solution and its dependence on polymer and particle concentrations.

Polymer processing benefits from the use of time–temperature superposition (TTSP), whereby the linear viscoelasticity of polymers can often be reduced to a master curve (Baumgärtel and Willenbacher 1996; Ferry 1980) over a range of temperatures and deformation frequencies. Similarly, polymer solutions within the concentrated regime have been shown to exhibit time–concentration superposition (TCSP) (Baumgärtel and Willenbacher 1996; Ferry 1980; Schausberger and Ahrer 1995). In the latter, concentration effects on the entanglement density and dominant relaxation time can be reduced to an underlying master curve. This reduction reflects the common underlying mechanisms responsible for the viscoelasticity. In addition to the obvious savings in data management, reduction to an underlying universal, viscoelastic spectrum is helpful both for measuring the rheology in a larger experimental window and for the prediction of the viscoelasticity at state points not actually measured. Likewise, the rheology of weakly attracting colloidal suspensions at different volume fractions or interaction energies, within a certain range, can be superimposed to reflect the commonality in the underlying viscoelasticity (Trappe and Weitz 2000).

The addition of nanoparticles to polymers and polymer solutions should significantly modify the viscoelasticity of the polymer or polymer solution if the particles strongly interact with the polymer. However, even relatively weakly interacting nanoparticles can have significant and nontrivial effects on the polymer's rheology because of their high surface-to-volume ratio and similar sizes (Mackay et al. 2003). As it is becoming increasingly common to add nanoparticles into polymers and polymer solutions to either enhance or impart desired properties to the resulting mixture, a systematic approach that could facilitate rheological measurements, their correlation and possible prediction is desirable.

The ternary mixture with laponite nanoclay dispersed in aqueous solutions of poly(ethylene oxide) (PEO), henceforth referred to as PWL mixture, is a model polymer–nanoclay dispersion that has received sufficient attention to make it both of academic and practical interest. PWL mixtures, with or without the presence of counterions, have been studied extensively at a wide range of PEO concentration through rheology, SANS and molecular modeling. At concentrations greater than 2 wt.%, aqueous laponite dispersions form a thixotropic gel with time (Willenbacher 1996). Monte Carlo simulations (Dijkstra et al. 1995) of laponite gels suggest a “house of cards” structure driven by

electrostatic attraction between oppositely charged edges and faces of the laponite discs (van Olphen 1977). Other structural models have been proposed to explain the structure and properties of laponite gels (Schmidt et al. 2002). The introduction of water-soluble polymers is known to retard or inhibit the gelation kinetics (Mongondry et al. 2004; Sardinha and Bhatia 2002a,b). The structure formation with time causes a significant change in rheology over days (Sardinha and Bhatia 2002a,b), such that ageing must be accounted for in any quantitative experimental study. Phase behavior studies and rheology of PWL system delineate the boundary within which PWL mixtures shear thicken reversibly to form ‘shake gels’ (Feller et al. 2004; Pozzo and Walker 2004; Zebrowski et al. 2003). Flow-birefringence studies revealed that upon shear the laponite discs orient along the flow direction (Schmidt et al. 2000; Schmidt et al. 2002).

SANS investigations show that PEO adsorbs to and can bridge between laponite particles, leading to the formation of a polymer–nanoparticle network in solution (Feller et al. 2004; Lal and Auvray 2001; Nelson and Cosgrove 2004; Pozzo and Walker 2004; Schmidt et al. 2000). Therefore, it can be expected that the addition of laponite particles to semi-dilute and concentrated PEO solutions will add structure to the solution and increase the viscoelasticity. This change could result in an increase in the effective entanglement density through PEO–laponite bridging interactions. However, adsorption onto laponite particles could also remove PEO chains from the entanglement network. Consequently, it is not known a priori whether such ternary mixtures will be rheologically “simple” so as to be represented by an underlying viscoelastic master curve. Here, we explore this by performing rheological investigations on a series of model PEO–laponite aqueous solutions covering a relevant and interesting range of compositions and temperatures.

Experimental

PEO (Scientific Polymer Products) with reported nominal $MW=9\times 10^5$ g/mol (PDI=2.4), laponite RD (Southern Clay Products) and deionized water with a resistivity of $18.3\text{ M}\Omega^{-\text{cm}}$ were used as supplied. PEO (6.62 and 8.0 wt.%) was added to deionized water in plastic bottles and sealed. The bottles were shaken vigorously to completely disperse the PEO. Three days were allowed for the complete dissolution of PEO in water during which the solutions were placed on a rotating mixer for gentle mixing. The aqueous PEO solutions, referred to as PW solutions henceforth, of lower concentrations were prepared by diluting either of the two stocks with an additional amount of deionized water, after which, the diluted samples were mixed for a day. Laponite (1.5 and 2.2 wt.%) was added to deionized water and shaken vigorously for a few minutes and then sonicated for ~30 min using a probe sonicator with

simultaneous mixing using a magnetic stirrer bar. Because laponite dispersions age, these were used within 2 h of sonication to prepare the PWL mixtures as discussed below.

The PWL mixtures of desired concentrations were prepared in glass vials from stock solutions of PEO and laponite dispersions by mixing 6.62 wt.% PEO solution with 1.5 wt.% laponite dispersion and mixing 8 wt.% PEO solution with 2.2 wt.% laponite dispersion in different weight ratios. The PWL samples were stirred briefly and then mixed on a vibrating mixer for a minimum of ~ 24 h. The PWL mixtures were optically clearer than neat PW solutions but some of the mixtures with higher laponite concentrations formed colorless gel-like agglomerates that settled with time. These agglomerates are characteristic of this system (Mongondry et al. 2004) and were fully re-dispersed by hand mixing prior to rheological measurement, i.e., all reported rheological data is on homogeneous samples. Furthermore, we note that the PWL mixtures are significantly more concentrated in polymer than those that form “shake gels” (Pozzo and Walker 2004; Zebrowski et al. 2003).

The shear rheology was measured using concentric cylinder geometry (CC27) on a MCR500 (Paar Physica) with a solvent trap to avoid evaporation and peltier temperature control ($\pm 0.03^\circ\text{C}$). Amplitude sweeps were performed to limit the frequency sweep measurements in the linear viscoelastic regime. The reported data was obtained for frequencies from 0 to 100 rad/s performed in controlled strain mode with a strain amplitude of 10%. The data was processed using the manual shifting mode of IRIS 8.04 program (Winter and Mours 2004) to perform superpositions (TTSP and TCSP) and spectrum calculations.

Limited ageing studies were performed on a PW solution (5 wt.%), a PWL mixture (3.69% P/1.18% L (PWL6)) and a laponite dispersion in water (2.7 wt.%). In the following discussion, “day 1” refers, respectively, to (1) the day of preparation of laponite dispersion, (2) the third day after the initial mixing of PEO and water to make PW solutions, and (3) 1 day after mixing the laponite and PW stock solutions to prepare the PWL mixtures. The shear viscosity and the frequency sweep of the PW solution (not shown here) was observed to be identical over a period of 40 days and, therefore, did not show evidence of ageing. The shear rate sweeps measured over 45 days on the laponite dispersion are shown in Fig. 1, with each curve measured on a freshly loaded sample. Just after preparation, this dispersion exhibited a low, nearly Newtonian viscosity. Within 3 days, an effective yield stress was evident, which continued to increase slowly with time. The amplitude sweep of this solution exhibited a maximum in the loss modulus, G'' , at high strains indicating a development of structure as previously reported by Willenbacher (1996).

Figure 2 shows the viscosity measurements performed in ascending (up to 500 s^{-1}) and descending sweeps on the PWL6 mixture. Similar to the laponite dispersions, the PWL6 (3.69% P/1.18% L) mixture also showed a gradual

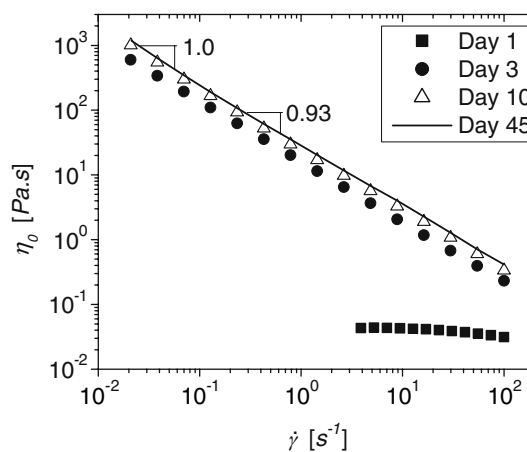


Fig. 1 Shear viscosity for 2.67 wt.% laponite dispersion measured over 45 days

increase in η with time, but the rate of increase was less than that for the corresponding laponite dispersion. This is consistent with recent reports that PEO retards the gelation kinetics of laponite dispersions (Sardinha and Bhatia 2002a,b). Further, the viscosity was observed to be substantially lower upon descending from high shear rates, which indicates partial shear redispersion of the structure. Also, in contrast to the laponite dispersion, the amplitude sweep for this PWL mixture was found to be qualitatively similar to that of a comparable PW with no maximum in G'' .

Except for ageing studies, where we deliberately sought information on how the system changes with time, all the other reported measurements were carried out with pre-sheared PWL mixtures within 1 to 4 days after preparation. Thus, the measured rheology was found to be reproducible and the differences in the observed rheology are a consequence of the differences in composition and not due to sample ageing.

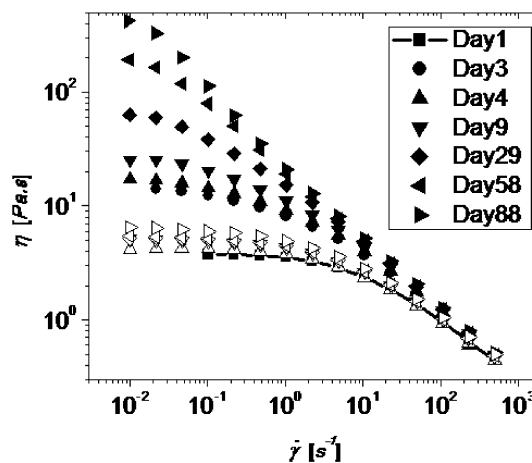


Fig. 2 Shear viscosity of PWL6 (3.69% P/1.18% L) at 25°C measured over 88 days (ascending and descending shear rates are represented by filled and empty symbols, respectively)

Results

Rheology of PEO–water solutions

PW solutions of 12 different concentrations, as indicated in Table 1, were prepared for the rheological characterization. The samples were designed to span the semi-dilute to concentrated regimes so as to be of practical importance as well as to explore the suitability of the two different concentration regimes for TTSP and TCSP. For PEO–water system, the Mark–Houwink–Sakurada equation for PEO of $MW=1 \times 10^5$ g/mol is given as (Polymer Handbook, 4th ed., 1999).

$$[\eta] = 0.0449MW^{0.67} \quad (1)$$

Using this expression for PEO of $MW=9 \times 10^5$ g/mol (used here), the concentrations, c^* and c^{**} , are given approximately as

$$c^* = \frac{1}{[\eta]} = 0.0023 \frac{\text{g}}{\text{ml}} \quad \text{and} \quad c^{**} \approx 8c^* = 0.0183 \frac{\text{g}}{\text{ml}}$$

The density of PEO and water are both close to 1 g/cm^3 , so these values correspond to :

$$c^* = 0.23 \text{ wt.} \% \quad \text{and} \quad c^{**} = 1.83 \text{ wt.} \% \quad (2)$$

Viscosity and concentration regimes

The measured shear viscosities of the PW solutions are shown in Fig. 3, where a pseudo-Newtonian plateau at low γ is followed by significant shear thinning. Also shown in Fig. 3 is the complex viscosity, η^* , vs. angular frequency, ω , which overlaps with the viscosity curve in the low

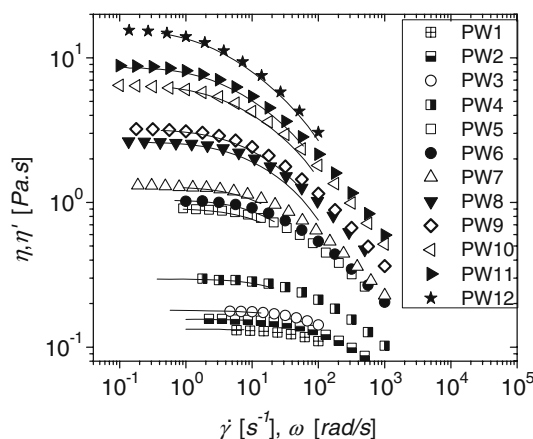


Fig. 3 Steady shear viscosity and validation of Cox–Merz rule for PW solutions at 25°C (symbols—steady shear viscosity vs. shear rate, lines—complex viscosity vs. angular frequency)

frequency limit, thereby validating the extended Cox–Merz rule for the PW solutions both in semi-dilute and concentrated regimes.

The zero shear viscosity, η_0 , increases with PEO concentration, c (Fig. 4), in quantitative correspondence with published data for the same system (Fong et al. (1999)). The change in slope of η_0 vs. c on a log–log plot from 2.4 to 5.0 occurs at a concentration of about 3.2 wt.% PEO. Based on the aforementioned calculations, we identify this as the transition from the semi-dilute to the concentrated, entangled regime. The difference with the calculated value of c^{**} (expression 2) is likely to be due to the large molecular weight polydispersity ($=3.5$) in the PEO. The zero shear viscosity is given by

$$\eta_0 = (0.0013 \pm 0.0009)c^{(5.0 \pm 0.4)} \quad (3)$$

in the concentrated regime.

Table 1 PW solutions prepared for rheological characterization

| Solution | PEO (wt.%) |
|----------|------------|
| PW1 | 2.24 |
| PW2 | 2.37 |
| PW3 | 2.52 |
| PW4 | 3.10 |
| PW5 | 3.74 |
| PW6 | 3.85 |
| PW7 | 4.00 |
| PW8 | 4.50 |
| PW9 | 5.00 |
| PW10 | 5.50 |
| PW11 | 6.00 |
| PW12 | 6.50 |

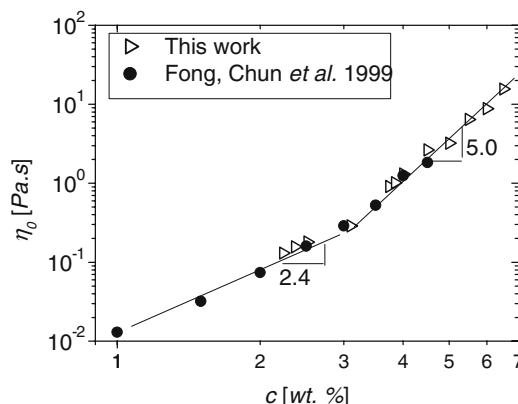


Fig. 4 Concentration regimes of PW solutions as defined by the zero-shear viscosity at 25°

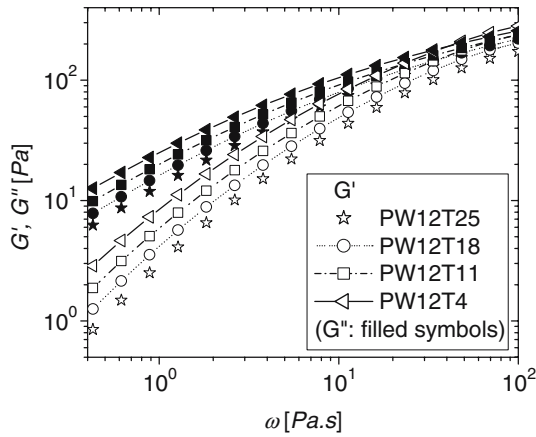


Fig. 5 Dynamic moduli of PW12 at 4, 11, 18 and 25°C

Time–temperature superposition

As discussed by Baumgärtel and Willenbacher (1996), superposition should be possible with the rheology of polymer solutions in the concentrated regime, namely PW5 to PW12. All of these samples exhibited a nearly Maxwellian response with appreciable storage modulus. Figure 5 shows the frequency sweeps for PW12 measured at four temperatures, namely, 4, 11, 18 and 25°C. In the legends, the name of sample is followed by the letter T (for temperature) and the measurement temperature in degrees Celsius. Figure 6 shows the same data after time–temperature superposition (TTSP) referenced to 25°C. As anticipated, only horizontal (time) shifting was required as the vertical shift factors, $b_T = T_{\text{ref}} \rho_{\text{ref}} / T \rho$, are expected to be unity for such a limited temperature range. As PW12 superimposes well, it is a thermorheologically simple fluid over this limited temperature range. The master curve in Fig. 6 is denoted by the same symbol as used to denote the reference curve in Fig. 5 as a reminder that the master curve is only an extension of the reference curve in a larger

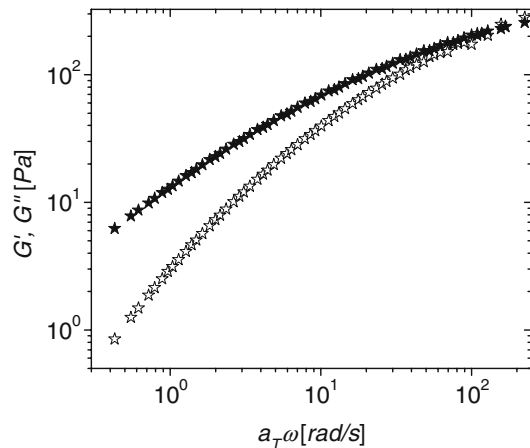


Fig. 6 TTSP master curve of PW12 referenced to 25°C

Table 2 Horizontal TTSP shift factors for PW10, PW11 and PW12

| Solution | T (°C) | a_T |
|----------|----------|-------|
| PW10 | 25 | 1 |
| PW10 | 20 | 1.2 |
| PW10 | 15 | 1.46 |
| PW10 | 10 | 1.79 |
| PW11 | 25 | 1 |
| PW11 | 18 | 1.3 |
| PW11 | 11 | 1.71 |
| PW11 | 4 | 2.32 |
| PW12 | 25 | 1 |
| PW12 | 18 | 1.28 |
| PW12 | 11 | 1.68 |
| PW12 | 4 | 2.26 |

experimental (in this case, frequency) window. Similarly, all the other master curves discussed later are represented by the symbols used for the reference curve during superposition. Shifting a low temperature data onto a higher temperature data extends the latter into high frequency domain as can be seen by comparing Figs. 5 and 6. TTSP was also performed for samples PW10 and PW11 with similar results as seen for PW12.

The shift factors resulting from the TTSP of PW10, PW11 and PW12 data are shown in Table 2 and plotted in Fig. 7. To gain insight into the molecular processes contributing to the viscosity and to predict the rheology at any temperature within the range of measurement temperatures, it is of interest to correlate the shift factors, a_T , with temperature. The glass transition temperature, T_g , of the PW solutions were estimated by the Gordon–Taylor equation using the Simha–Boyer rule (Hancock and Zografis 1994) with the following values for the individual T_g and density, ρ : $T_{g,\text{PEO}}=218$ K, $T_{g,\text{water}}=135$ K, $\rho_{\text{PEO}}=1.1$ g/cm³ and $\rho_{\text{water}}=1$ g/cm³. All the measurement temperatures employed were greater than (T_g+100) K of any solution and,

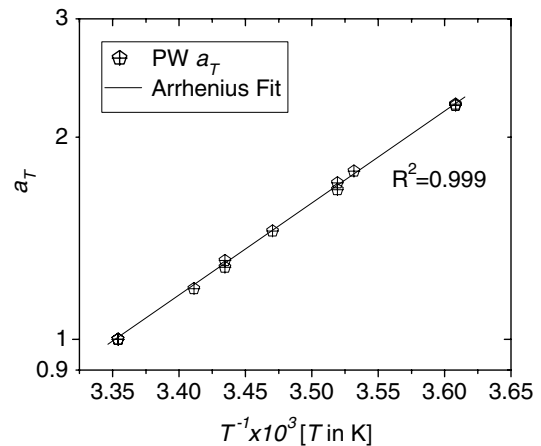


Fig. 7 Horizontal shift factors, a_T , for TTSP of PW10, PW11 and PW12

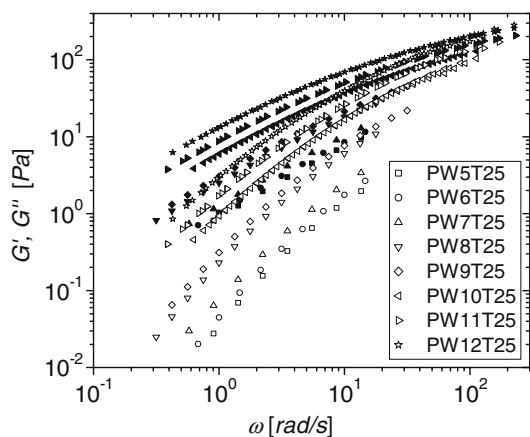


Fig. 8 Dynamic moduli of PW solutions in the concentrated regime: PW5 to PW12 (PW10, PW11 and PW12 from their TTSP master curves) at 25°C

therefore, the TTSP shift factors are expected to follow the Arrhenius equation,

$$a_T = \exp \left[\frac{-\Delta H}{R} \left(\frac{1}{T} - \frac{1}{T_{ref}} \right) \right] \quad (4)$$

which is observed in Fig. 7. The activation enthalpy for flow is found to be independent of concentration,

$$-\Delta H = (26.4 \pm 0.8) \text{ kJ/mol} \quad (5)$$

This is greater than that of the solvent, water (17 kJ/mol) (Welty et al. 1984), and, therefore, consistent with the fact that the viscoelasticity is due to polymer–polymer interactions.

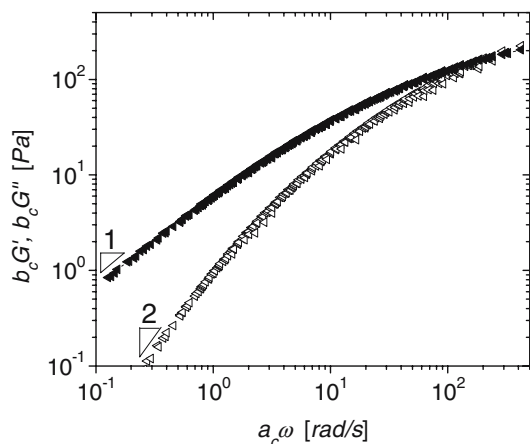


Fig. 9 TCSP master curve of the PW solutions referenced to 5.5 wt. % PEO (PW10) at 25°C

Table 3 Shift factors for TCSP of PW solutions

| Solution | a_c | b_c |
|----------|-------------------|-------------------|
| PW3 | 0.03 ^a | 1.68 ^a |
| PW5 | 0.168 | 1.26 |
| PW6 | 0.186 | 1.2 |
| PW7 | 0.234 | 1.17 |
| PW8 | 0.457 | 1.15 |
| PW9 | 0.525 | 1.07 |
| PW10 | 1 | 1 |
| PW11 | 1.41 | 0.912 |
| PW12 | 1.86 | 0.794 |

^aValues were found by correlating a_c and b_c with concentration

Time–concentration superposition

The dynamic moduli of PW solutions in the concentrated regime, namely, PW5, PW6, ..., PW9 measured at 25°C are shown in Fig. 8 along with the TTSP master curves for samples PW10, PW11 and PW12. The PW solutions belonging to the semi-dilute concentration regime, namely, PW1, PW2, PW3 and PW4, did not show any appreciable elasticity and, therefore, were not considered further. As is apparent from Fig. 8, concentrated solutions exhibit similar rheology and, therefore, could be shifted horizontally and vertically to create a concentration master curve referenced to the 5.5 wt.% PW solution, (i.e., PW10 at 25°C, shown in Fig. 9). Here, vertical shifting was also required because the vertical shift factors depend upon the concentration (Baumgärtel and Willenbacher 1996; Ferry 1980).

The shift factors resulting from the TCSP of PW5 to PW12 data are shown in Table 3 and plotted in Fig. 10. Also shown for comparison are the shift factors calculated using the scalings expected for ideal Gaussian chains as reported by Baumgärtel and Willenbacher (1996) ($a_c \sim c^{3.5}$, $b_c \sim c^{-2.2}$).

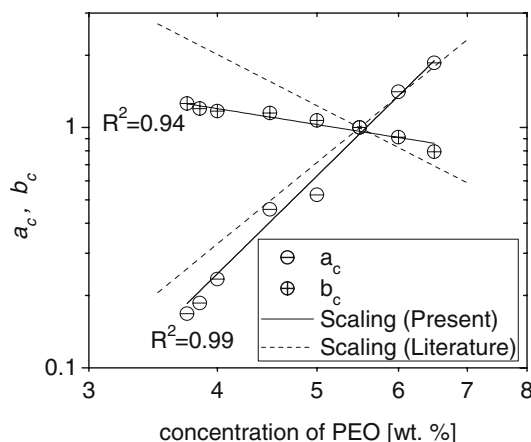


Fig. 10 Horizontal and vertical TCSP shift factors for PW5 to PW12 and their comparison with the scaling for ideal solutions (Baumgärtel and Willenbacher 1996)

Table 4 PWL mixtures prepared for rheological characterization

| Ternary mixture | PW base solution | Group | P (%) | L (%) | W (%) | 100×P/(P+W) | 100×L/(L+P) | Mixing time (day) |
|-----------------|------------------|-------|-------|-------|-------|-------------|-------------|-------------------|
| PWL1 | PW3 | 1 | 2.49 | 0.94 | 96.57 | 2.51 | 27.31 | 2 |
| PWL2 | PW5 | 2 | 3.71 | 0.66 | 95.63 | 3.73 | 15.09 | 1 |
| PWL3 | PW8 | 3 | 4.48 | 0.49 | 95.04 | 4.50 | 9.79 | 1 |
| PWL4 | PW10 | 4 | 5.49 | 0.26 | 94.26 | 5.50 | 4.48 | 2 |
| PWL5 | PW3 | 1 | 2.48 | 1.52 | 96.00 | 2.52 | 38.00 | 2 |
| PWL6 | PW5 | 2 | 3.69 | 1.18 | 95.12 | 3.74 | 24.28 | 1 |
| PWL7 | PW8 | 3 | 4.45 | 0.97 | 94.57 | 4.50 | 17.96 | 3 |
| PWL8 | PW10 | 4 | 5.46 | 0.70 | 93.84 | 5.50 | 11.33 | 4 |
| PWL9 | PW12 | 5 | 6.47 | 0.42 | 93.10 | 6.50 | 6.10 | 2 |

Our TCSP shift factors, a_c and b_c , also follow power law correlations with concentration given as

$$a_c = (6.7 \times 10^{-4} \pm 2.6 \times 10^{-4})c^{(4.2 \pm 0.2)} \tag{6}$$

$$b_c = (3.25 \pm 0.38)c^{(-0.72 \pm 0.08)} \tag{7}$$

This difference in scaling can be rationalized in terms of solvent quality effects, as will be discussed shortly.

Rheology of PEO–water–laponite solutions

The concentrations of PWL mixtures (PWL1 (2.49% P/0.94% L) to PWL9 (6.47% P/0.42% L)) are listed in Table 4. These concentrations were chosen to investigate the effects of adding laponite to concentrated PW solutions (PW base solutions). As shown in Table 4, five different

groups were formed with each group containing a PW base solution and corresponding PWL mixtures with the PEO to water ratio ($100P/(P+W)$) equal to the PW base solution. Thus, successive mixtures in each group can be compared to the corresponding neat PW base solution in the group to determine the effects of laponite addition upon the rheology of PW solutions.

Effect of laponite on viscosity

The shear thinning response of the PWL mixtures is shown in Fig. 11 along with the corresponding dynamic viscosity $\eta^*(\omega)$, which are in reasonable agreement. As expected of the PWL mixtures containing PEO in excess, the shear viscosity is qualitatively similar to the PW solutions. Quantitative comparison of Figs. 3 and 11 shows that at the same total solids loading, the viscosity is higher for higher laponite concentrations (e.g., PW7 and PWL5 (2.48% P/1.52% L) are both 96% water, but PWL5 is about three times as viscous).

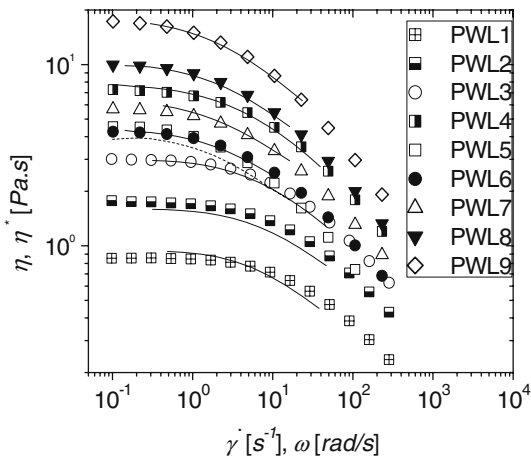


Fig. 11 Steady shear viscosity and validation of Cox–Merz rule for PWL mixtures at 25°C (symbols—viscosity vs. shear rate, lines—complex viscosity vs. angular frequency)

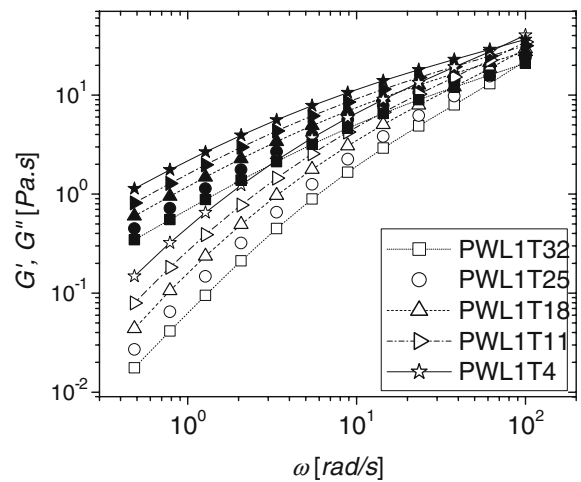


Fig. 12 Dynamic moduli of PWL1 (2.49% P/0.94% L) at 4, 11, 18, 25 and 32°C

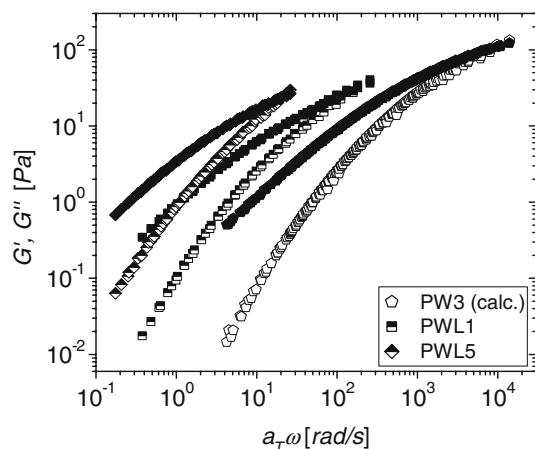


Fig. 13 TTSP master curve of PWL1 (2.49% P/0.94% L), TTSP master curve of PWL5 (2.48% P/1.52% L) and the calculated PW3 curve all referenced to 25°C

Time–temperature superposition

The frequency sweep measurements were performed for laponite-filled systems at five different temperatures each, namely, 4, 11, 18, 25 and 32°C. Upon TTSP of the data referenced to 25°C, the data superimposed well showing that the PWL mixtures are thermorheologically simple, at least, in this limited temperature range. Once again, no vertical shifting was required for TTSP because of the narrow temperature range. As an example, the dynamic shear moduli of PWL1 (2.49% P/0.94% L) are shown at five different temperatures in Fig. 12. It is remarkable to note that unlike its corresponding base solution, PW3, the PWL1 (2.49% P/0.94% L) mixture with less than 1 wt.% laponite showed a substantial elasticity and a Maxwellian behavior. Shown in Fig. 13 is the TTSP master curve of PWL1 referenced to 25°C, the TTSP master curve of PWL5 (2.48% P/1.52% L) referenced to 25°C, and the curve for PW3 predicted from the PW master curve shown in Fig. 9 using the shift factor correlations, 6 and 7. This is a hypothetical prediction by extrapolation from the PW master curve made for purposes of comparison; sample PW3 does not exhibit this viscoelasticity in experiment as it falls in the semi-dilute regime.

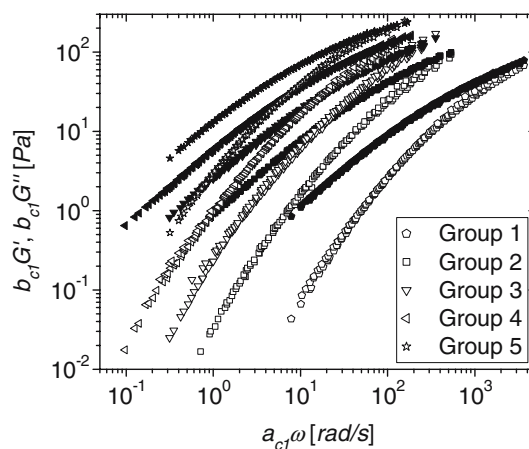


Fig. 14 Groupwise TCSP (TCSP₁) master curves of PWL mixtures at 25°C referenced to PW base solution in each group

Listed in Table 5 are the TTSP shift factors (master curves not shown for brevity), a_T , for all PWL samples along with the activation energy for flow, obtained by fitting a_T vs. T data of PWL mixtures to Arrhenius equation Eq. (4). The fitted values can be used to predict a_T , and hence the rheology of PWL1 (2.49% P/0.94% L) to PWL9 (6.47% P/0.42% L) in the range of 4 to 32°C.

First time–concentration superposition

As shown in Fig. 13 for group 1, the viscoelastic spectra for samples in the same group had a similar shape but were displaced as the laponite content was increased. Therefore, the curves of PWL mixtures in a group were superimposed onto curves for the respective PW base solutions belonging to that particular group. Figure 14 shows the five pairs of G' and G'' master curves, one for each group. This shifting is referred to as TCSP₁ henceforth and the shift factors referred to as a_{c1} and b_{c1} are listed in Table 6. As within each group the PEO–water concentration is fixed, this first TCSP (TCSP₁) accounts for the changes associated with the addition of laponite to a base PW solution. Compar-

Table 5 Horizontal TTSP shift factors and activation energy of flow for PWL mixtures

| | 32°C | 25°C | 18°C | 11°C | 4°C | $-\Delta H$ (kJ/mol) |
|------|-------|------|------|------|------|----------------------|
| PWL1 | 0.778 | 1 | 1.32 | 1.81 | 2.57 | 30.0 |
| PWL2 | 0.768 | 1 | 1.33 | 1.81 | 2.54 | 30.0 |
| PWL3 | 0.772 | 1 | 1.32 | 1.78 | 2.48 | 29.3 |
| PWL4 | 0.771 | 1 | 1.34 | 1.77 | 2.41 | 28.6 |
| PWL5 | 0.843 | 1 | 1.24 | 1.61 | 2.18 | 23.9 |
| PWL6 | 0.793 | 1 | 1.29 | 1.73 | 2.37 | 27.5 |
| PWL7 | 0.801 | 1 | 1.3 | 1.74 | 2.42 | 27.8 |
| PWL8 | 0.787 | 1 | 1.29 | 1.72 | 2.34 | 27.4 |
| PWL9 | 0.796 | 1 | 1.28 | 1.67 | 2.24 | 26.0 |

Table 6 Shift factors for the TCSP(TCSP₁) of PWL mixtures on their respective PW base solutions

| | | a_{c1} | b_{c1} |
|---------|------|----------|----------|
| Group 1 | PW3 | 1 | 1 |
| | PWL1 | 20.9 | 2.45 |
| | PWL5 | 81.3 | 2.24 |
| Group 2 | PW5 | 1 | 1 |
| | PWL2 | 2.95 | 1.62 |
| | PWL6 | 9.95 | 2.01 |
| Group 3 | PW8 | 1 | 1 |
| | PWL3 | 1.45 | 1.32 |
| | PWL7 | 4.37 | 1.74 |
| Group 4 | PW10 | 1 | 1 |
| | PWL4 | 1.26 | 1.07 |
| | PWL8 | 1.95 | 1.23 |
| Group 5 | PW12 | 1 | 1 |
| | PWL9 | 1.35 | 1.15 |

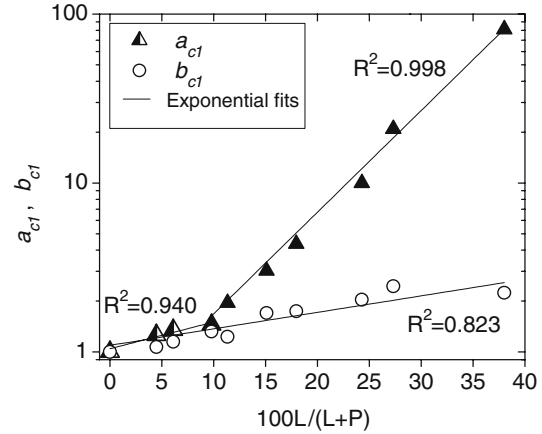
The required rheology of PW3 for TCSP of group 1 mixtures was predicted from the PW TCSP master curve shown in Fig. 9 with shift factors (Eqs. 6 and 7) extrapolated to the concentration of PW3

isons of master curves between groups compare samples with different concentrations of polymer.

Upon further inspection, and as shown in Fig. 15, it is apparent that the shift factors, a_{c1} and b_{c1} , are strong functions of the percentage of laponite in the mixture on a water-free basis tabulated as $100L/(L+P)$ in Table 4. The shift factor, a_{c1} , was found to conform to a piecewise exponential function Eq. (8), whereas the shift factor, b_{c1} , was described well by a single exponential function Eq. (9).

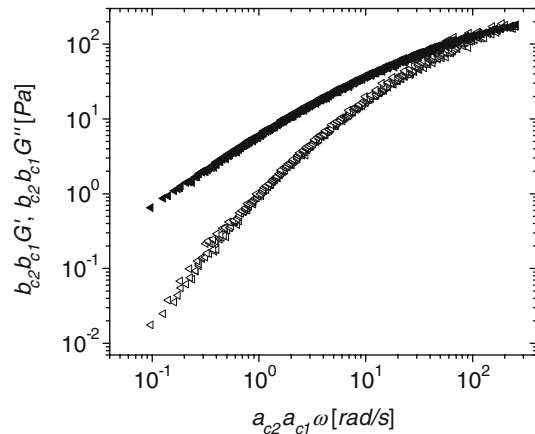
$$a_{c1} = \begin{cases} (1.04 \pm 0.05) \exp \left[(0.036 \pm 0.007) \left(\frac{100L}{(L+P)} \right) \right], & 0 \leq \frac{100L}{(L+P)} < 10 \\ (0.42 \pm 0.08) \exp \left[(0.139 \pm 0.005) \left(\frac{100L}{(L+P)} \right) \right], & \frac{100L}{(L+P)} \geq 10 \end{cases} \quad (8)$$

$$b_{c1} = (1.09 \pm 0.10) \exp \left[(0.022 \pm 0.004) \left(\frac{100L}{(L+P)} \right) \right] \quad (9)$$

**Fig. 15** TCSP shift factors for groupwise shifting (TCSP₁) of PWL TTSP master curves at 25°C on the respective PW base solutions

Complete time–concentration superposition

The master curves formed by shifting the various laponite concentrations onto the base PW solutions (i.e., the results of TCSP₁) are observed to successfully TCSP. This TCSP is shown in Fig. 16 and denoted by TCSP₂. The group 4 master curve was chosen as reference for TCSP₂. This is equivalent to shifting the curves for base solutions PW3, PW6, PW8 and PW12 onto PW10 chosen as reference. Therefore, the shift factors, a_{c2} and b_{c2} , for TCSP₂ should be and were found identical to the shift factors that result from the TCSP of PW solutions as listed in Table 3. By the same reasoning, the relaxation spectrum of the PW TCSP master curve is found (not shown here) to reproduce the PWL master curve obtained after TCSP₂.

**Fig. 16** Complete TCSP (TCSP₂) master curve of PWL mixtures at 25°C referenced to group 4 (or PW10)

Discussion

Reducing temperature reduces molecular motion and, hence, increases the relaxation time of the entangled polymer chain. This is the basis for the corresponding increase in the TTSP shift factors, a_T , for both neat and laponite-filled PW solutions. Over this limited temperature range, however, the density does not change significantly (Ferry 1980) so vertical shifting is not required.

TCSP shift factors for the PW solutions, $a_{c1} \propto c^\alpha$ and $b_{c1} \propto c^\beta$, are related to the concentration dependence of the zero shear viscosity $\eta_0 \propto c^\delta$ by $\delta = \alpha - \beta$. The value of $\alpha - \beta = 4.92 \pm 0.28$ from (Eqs. 6 and 7) is in agreement with the measured value of $\delta = 5.0 \pm 0.4$ Eq. (3).

The concentration scaling of PW TCSP shift factors differ from those proposed by Baumgärtel and Willenbacher (1996) for polystyrene–ethylbenzene systems. The scaling exponent of b_c is -0.72 is found here in comparison to -2.2 , which implies a weaker dependence of the plateau modulus upon the concentration of polymer for the PW solutions as compared to ideal solutions. This can be understood as an effect of solvent quality. Water is a good solvent for PEO around 25°C as observed from the measured second virial coefficient, $A_2 = 1.2 \times 10^{-3} \text{ mL mol/g}^2$ at 30°C (Devanand and Selser 1991) and a favorable Flory–Huggins interaction parameter, $\chi = 0.12 (= -w/RT)$ at 30°C in the range between 5 and 40 wt% PEO (2,290 g/mol) solution in water (Kjellander and Florin 1981). As the polymer concentration increases, the solvent quality should tend toward theta conditions. Hence, the swollen PEO chains in good solvent will reduce in coil size with increasing polymer concentration. Thus, adding PEO will not lead to the expected increase in chain overlap and, hence, a weaker concentration dependence of the plateau modulus (and hence the vertical shift factor b_c) is expected. The higher-than-expected scaling exponent for the relaxation time (a_c) can be rationalized through an increase in molecular friction with increasing polymer concentration due to specific polymer–polymer segment interactions mitigated by hydrogen bonding. Indeed, hydrogen-bonded clusters have been reported for similar PEO water solutions (Hammouda et al. 2002, 2004; Ho et al. 2003).

Adding laponite to the base PW solutions increased the relaxation time yet *decreased* the plateau modulus. This counter-intuitive observation is a consequence of the specifics of the PEO–laponite interactions. The concentration variable, $100L/(L+P)$ was observed to correlate the TCSP₁ shift factors over the different polymer and laponite concentrations. This variable is closely related to the parameter Γ_t proposed earlier to characterize the phase behavior of PWL solutions (Pozzo and Walker 2004). Assuming, the specific adsorption surface area provided by

the laponite discs for PEO adsorption to be $s \text{ m}^2/\text{g}$, Γ_t^{-1} is given as

$$\Gamma_t^{-1} = \frac{sL}{100P} \frac{m^2}{mg} \quad (10)$$

where, P and L denote the weight percent of PEO and laponite in a PWL mixture. For small laponite concentrations, as is the case here, the two parameters are nearly proportional. Therefore, the trend in the shift factors, a_{c1} and b_{c1} , with the relative laponite concentration variable, $100L/(L+P)$, can be understood simply in terms of the surface area provided by laponite per unit mass of PEO present.

The increase in the shift factor, b_{c1} , with $100L/(L+P)$ reflects the corresponding reduction in the plateau modulus apparent in Fig. 13. A decrease in the plateau modulus with the addition of laponite particles to the PW base solutions suggests that PEO adsorbs to the laponite, thus reducing the entanglement density. However, some bridging must also be evident, as despite this reduction in plateau modulus, there is a net increase in the longest relaxation time as characterized by a_{c1} (Fig. 15). To confirm this proposition, the gel and the solution phases of two representative PWL mixtures, PWL5 and PWL6, were separated by centrifugation at 1,200 rpm for 15 min and the concentration of both phases was measured by thermogravimetric analysis (TGA) as listed in Table 7. The gel phase contains a higher concentration of both PEO and laponite, which is consistent with the aforementioned hypothesis. The removal of PEO from the network to form gel particles is a relatively small effect, however, as the gel phase is only about a fifth of the sample. This confirms that the removal of PEO chains from the entanglement network by adsorption onto laponite is a modest effect. The presence of some bridging, adsorbed PEO chains on laponite, in the solution phase increases the dominant relaxation time (and hence a_{c1}) as seen in Fig. 13.

Figure 15 demonstrates that above the value $100(L+P)/\approx 10$, the addition of laponite greatly increases the longest relaxation time for the polymer solution. It has been

Table 7 Weight and concentration of solution and gel phases of PWL5 (2.48% P/1.52% L) and PWL6 (3.69% P/1.18% L) by TGA analysis

| | Overall concentration (wt.%) | Solution phase weight and concentration (wt.%) | Gel phase weight and concentration (wt.%) |
|------|------------------------------|--|---|
| PWL5 | $P=2.48,$ $L=1.52$ | (27.24 g) $P=2.43, L=1.02$ | (5.64 g) $P=2.78, L=2.76$ |
| PWL6 | $P=3.69,$ $L=1.18$ | (22.97 g) $P=3.38, L=0.79$ | (5.12 g) $P=4.27, L=1.82$ |

reported that ~1 wt.% PEO is capable of saturating the laponite surface in a 2-wt.% aqueous dispersion of laponite (Lal and Auvray 2000, 2001). Therefore, the laponite particles in our mixtures are expected to be saturated with adsorbed PEO. However, the likelihood of bridging relative to nonbridging polymer will depend upon the relative concentrations, i.e., at low relative laponite concentrations there is less probability of a chain adsorbing to multiple laponite particles. Whereas at higher laponite concentrations, polymer bridging is more likely and percolation of the bridge network is possible. Consequently, the change in behavior of the TCSPs with relative laponite concentration is interpreted to suggest changes in the structure of the adsorbed polymer layer and the likelihood of polymer bridging.

Conclusions

PEO–water solutions were observed to be thermorheologically simple in the concentrated solution regime over the limited temperature range of 4–32°C. However, unlike previous measurements for nearly ideal chains in theta solvents, aqueous PEO solutions exhibit a weaker increase in plateau modulus and a stronger increase in relaxation time with increasing polymer concentration. The former is qualitatively understood as a consequence of the good solvent quality whereas the latter is attributed to specific

hydrogen bonding interactions present in aqueous PEO solutions.

The addition of laponite to these solutions also yielded thermorheologically simple solutions (although ageing effects were observed over longer time scales), but with nontrivial concentration dependencies of the shift factors. Specifically, adding laponite was observed to decrease the plateau modulus while weakly increasing the relaxation time up to a critical relative concentration, whereupon the dominant relaxation time was observed to diverge rapidly. This complex behavior is interpreted as a competition between PEO adsorption on laponite removing PEO from the entanglement network vs. forming new bridging networks. Evidence of gel formation upon ageing within the solutions confirms this simple interpretation.

These results provide a practical framework for correlating rheological data on polymer–nanoparticle solutions and for predicting linear viscoelasticity of such solutions. They also illustrate the value in using a master curve analysis to derive microstructural insights from bulk rheological measurements.

Acknowledgements We are thankful to Dr. H. H. Winter, University of Massachusetts, for technical assistance using IRIS, and to Dr. Norbert Willenbacher (Uni, Karlsruhe) for useful discussions. Funding from the National Science Foundation (DMR-0210223) supported this work.

References

- Aranda P, Mosqueda Y, Perez-Capote E, Ruiz-Hitzky, E (2003) Electrical characterization of poly(ethylene oxide)–clay nanocomposites prepared by microwave irradiation. *J Polym Sci, Part B, Polym Phys* 41(24):3249–3263
- Baumgärtel M, Willenbacher N (1996) The relaxation of concentrated polymer solutions. *Rheol Acta* 35(2):168–185
- Brandup J, Immergut EH, and Grulke EA (eds) (1999) *Polymer Handbook*, 4th edn. Wiley, New York
- Casper CL, Stephens JS, Tassi NG, Chase DB, Rabolt JF (2004) Controlling surface morphology of electrospun polystyrene fibers: effect of humidity and molecular weight in the electrospinning process. *Macromolecules* 37(2):573–578
- Devanand K, Selser JC (1991) Asymptotic behavior and long-range interactions in aqueous-solutions of poly(ethylene oxide). *Macromolecules* 24(22):5943–5947
- Dijkstra M, Hansen JP, Madden PA (1995) Gelation of a clay colloid suspension. *Phys Rev Lett* 75(11):2236–2239
- Doeff MM, Reed JS (1998) Li ion conductors based on laponite/poly(ethylene oxide) composites. *Solid State Ionics* 115:109–115
- Drew C, Wang X, Samuelson LA, Samuelson JK (2003) The effect of viscosity and filler on electrospun fiber morphology. *J Macromol Sci, Part A* 40(12):1415–1422
- Feller JF, Bruzard S, Grohens Y (2004) Influence of clay nanofiller on electrical and rheological properties of conductive polymer composite. *Mater Lett* 58(5):739–745
- Ferry JD (1980) *Viscoelastic properties of polymers*. 3rd edn. Wiley, New York
- Fong H, Chun I, Reneker DH (1999) Beaded nanofibers formed during electrospinning. *Polymer* 40(16):4585–4592
- Greenblatt GD, Hughes L, Whitman DW (2004) Polymer–clay nanocomposite for extended release of active ingredient. *European Patent Applications*, EP 1470823
- Hammouda B, Ho D, Kline S (2002) SANS from poly(ethylene oxide)/water systems. *Macromolecules* 35(22):8578–8585
- Hammouda B, Ho DL, Kline S (2004) Insight into clustering in poly(ethylene oxide) solutions. *Macromolecules* 37(18):6932–6937
- Hancock BC, Zografis G (1994) The relationship between the glass-transition temperature and the water-content of amorphous pharmaceutical solids. *Pharm Res* 11(4):471–477
- Ho DL, Hammouda B, Kline SR (2003) Clustering of poly(ethylene oxide) in water revisited. *J Polym Sci, Part B, Polym Phys* 41(1):135–138
- Huang Z-M, Zhang Y-Z, Kotaki M (2003) A review on polymer nanofibers by electrospinning and their applications in nanocomposites. *Compos Sci Technol* 63(15):2223–2253
- Jayaraman K, Kotaki M, Zhang YZ, Mo XM, Ramakrishna S (2004) Recent advances in polymer nanofibers. *J Nanosci Nanotechnol* 4(1–2):52–65
- Kjellander R, Florin E (1981) Water-structure and changes in thermal-stability of the system poly(ethylene oxide)–water. *J Chem Soc, Faraday Trans I* 77:2053–2077

- Krikorian V, Casper C, Rabolt J, Pochan D (2004) Electrospinning of nanocomposite fibers based on poly(L-lactic acid) and organoclays. *Polym Mater Sci Eng* 90(51)
- Lal J, Auvray L (2000) Interaction of polymer with clays. *J Appl Crystallogr* 3(3, Pt. 1):673–676
- Lal J, Auvray L (2001) Interaction of polymer with discotic clay particles. *Mol Crystals Liq Crystals* 356: 503–515
- Mackay ME, Dao TT, Tuteja A, Ho DL, Van Horn B, Kim HC, Hawker CJ (2003) Nanoscale effects leading to non-Einstein-like decrease in viscosity. *Nat Mater* 2(11):762–766
- Majumdar DB, Thomas N, Schwark, Dwight W (2003) Clay–polymer nanocomposite coatings for imaging application. *Appl Clay Sci* 23(5–6):265–273
- McKee MG, Wilkes GL, Colby RH, Long TE (2004) Correlations of solution rheology with electrospun fiber formation of linear and branched polyesters. *Macromolecules* 37(5):1760–1767
- Megelski S, Stephens JS, Chase DB, Rabolt JF (2002) Micro- and nanostructured surface morphology on electrospun polymer fibers. *Macromolecules* 35(22):8456–8466
- Mongondry P, Nicolai T, Tassin JF (2004) Influence of pyrophosphate or polyethylene oxide on the aggregation and gelation of aqueous laponite dispersions. *J Colloid Interface Sci* 275(1):191–196
- Nelson A, Cosgrove T (2004) A small-angle neutron scattering study of adsorbed poly(ethylene oxide) on laponite. *Langmuir* 20(6):2298–2304
- Pozzo DC, Walker LM (2004) Reversible shear gelation of polymer–clay dispersions. *Colloids Surf, A Physicochem Eng Asp* 240(1–3):187–198
- Sardinha H, Bhatia SR (2002a). Controlling gel formation in clay dispersions via water-soluble polymer: viscoelasticity and kinetics of gel formation. Submitted to *RheoFuture Thermo Haake Young Scientists Award 2002*
- Sardinha H, Bhatia SR (2002b) Kinetics of gel formation in polymer–clay dispersions. Abstracts of Papers of the American Chemical Society 224:U526–U526
- Schausberger A, Ahrer IV (1995) On the time–concentration superposition of the linear viscoelastic properties of plasticized polystyrene melts using the free-volume concept. *Macromol Chem Phys* 196(7):2161–2172
- Schmidt G, Nakatani AI, Butler PD, Karim A, Han CC (2000) Shear orientation of viscoelastic polymer–clay solutions probed by flow birefringence and SANS. *Macromolecules* 33(20): 7219–7222
- Schmidt G, Nakatani AI, Han CC (2002) Rheology and flow-birefringence from viscoelastic polymer–clay solutions. *Rheol Acta* 41(1–2):45–54
- Sengupta AK, Spindler R, Darlington JW, Amcol International Corporation U (2002) Multifunctional particulate additive for personal care and cosmetic compositions. PCT Appl, WO 2002062310
- Smith DN, Goodman H, Buse WR, ECC International Ltd. U (1989) Thixotropic composition containing smectite clays for personal care products. EP 301065
- Theng BKG (1970) Interactions of clay minerals with organic polymers—some practical applications. *Clays Clay Miner* 18(6):357
- Trappe V, Weitz DA (2000) Scaling of the viscoelasticity of weakly attractive particles. *Phys Rev Lett* 85(2):449–452
- van Olphen H (1977) An introduction to clay colloid chemistry. Wiley, New York
- Welty JR, Wicks CE, Wilson RE (1984) Fundamentals of momentum, heat and mass transfer, 3rd edn. Wiley, New York, pp 772–773
- Willenbacher N (1996) Unusual thixotropic properties of aqueous dispersions of laponite RD. *J Colloid Interface Sci* 182(2):501–510
- Winter HH, Mours M (2004) <http://rheology.tripod.com/>
- Wong D (2004) Novel pharmaceutical formulations containing polymer clay composites. US Patent Appl, US 20044101559, 27 May 2004
- Zebrowski J, Prasad V, Zhang W, Walker LM, Weitz DA (2003) Shake-gels: shear-induced gelation of laponite–PEO mixtures. *Colloids Surf, A Physicochem Eng Asp* 213(2–3): 189–197